Available online at www.sciencedirect.com
ScienceDirect
Journal of the European Ceramic Society 27 (2007) 4509–4514
www.elsevier.com/locate/jeurceramsoc

Stability of $SrFeO_3$ based materials in the presence of SiO_x species in humid atmosphere at high temperatures and pressures

Ingeborg Kaus [a,1], Kjell Wiik [a], Marit Dahle [b], Morten Brustad [b], Siv Aasland [b,*]

[a] *Department of Materials Science and Engineering, Norwegian University of Science and Technology, 7491 Trondheim, Norway*
[b] *Statoil Research Centre, Statoil ASA, 7005 Trondheim, Norway*

Received 25 August 2006; received in revised form 16 March 2007; accepted 31 March 2007
Available online 12 June 2007

Abstract

Strontium silicate was found on the surface of $La_{0.2}Sr_{0.8}Fe_{0.79}Cr_{0.2}Mg_{0.01}O_3$ exposed to hydrogen containing humid atmospheres at 1000 °C and 30 bars. Silica originated from the furnace tube material and was transported via the gas phase as a gaseous silica hydrate. Fe and Sr were initially preferentially expelled from the perovskite grain boundaries to give Sr_2SiO_4 at the surface, along with a secondary Fe-rich phase and a $LaCrO_3$-rich grain boundary region. Eventually, Fe and Sr were drawn from the grains, leaving a porous structure. This investigation highlights the importance of avoiding Si sources near Sr-rich membranes in humid atmospheres at high temperatures.

Keywords: Perovskites; Membranes; SiO_2; Silicate; Chemical properties; (La, Sr)(Fe, Cr, Mg)O_3

1. Introduction

Oxygen membranes made from mixed conductors will transport oxygen electrochemically in an oxygen chemical potential gradient. They have potential applications as oxygen separation membranes for extraction of oxygen from air, e.g. for medical applications and production of syngas.[1–3] The main advantage of these membranes over membranes based on physical principles is the fact that they are only permeable to oxygen, giving 100% selectivity. The production of syngas occurs when methane as the fuel on one side reacts with oxygen that is transported through from the air side to form CO and H_2 gas, combining two operations into one, eliminating the need to separate oxygen from air prior to oxidation.[4,5]

A major challenge in all membrane applications is the stability of the materials in the severe operational conditions such as high temperature, large chemical potential gradients and corrosive reaction gases.[6] Three types of reactions may be identified: interface reactions between the different materials in the membrane system, reactions between membrane materials and the surrounding atmosphere, or decomposition of a material due to thermodynamic instability under operating conditions.[7,8] Any or all of these reactions may cause degradation of the performance of the membrane.

It is well known that silica should be avoided when making ceramic materials, as it is an excellent glass former and forms low-melting phases with many of the metal oxides common to these materials. Reactions with SiO_2 during operation are, however, not well known. Viitanen et al.[9] have reported on silica poisoning of $La_{0.6}Sr_{0.4}Co_{0.2}Fe_{0.8}O_3$ membranes, which was found to cause deterioration of the membrane performance over time.

During our investigation on the stability of the present perovskite material, strontium silicate was unexpectedly found on the surface of the material. The presence of strontium silicate was detected by a combination of SEM, IR and XRD analysis of the sample surface, and the Si-source was identified to be the furnace tube material, Manaurite XM, which contained 1.77% Si. Si is usually added to an alloy to inhibit corrosion of the metal, and will reside on the surface of the metal as SiO_2.

In order to reveal in more detail the effect on material stability having a rather dilute metallic Si source in the vicinity of our samples, we decided to conduct a more careful study of $La_{0.2}Sr_{0.8}Fe_{0.79}Cr_{0.2}Mg_{0.01}O_3$ in humid atmosphere at high temperatures and pressures. This perovskite material is chosen

* Corresponding author. Tel.: +47 97108469; fax: +47 73584965.
E-mail address: siaas@statoil.com (S. Aasland).
[1] Present address: SINTEF Materials and Chemistry, Sem Seelandsvei 12, 7465 Trondheim, Norway.

0955-2219/$ – see front matter © 2007 Elsevier Ltd. All rights reserved.
doi:10.1016/j.jeurceramsoc.2007.03.040

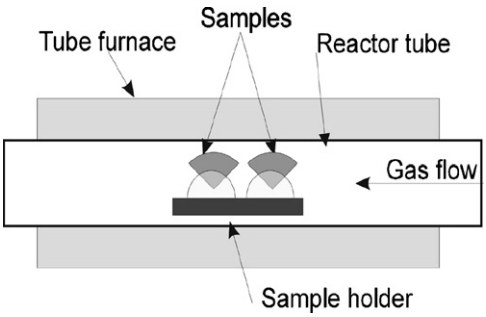

Fig. 1. Furnace construction.

for its potentially high oxygen flux combined with a high stability, and flux data for this composition and related compositions are presented in a separate paper.[12] The small amount of Mg was added to the perovskite in order to inhibit grain growth, and thus increase strength, during sintering. Stability of this material in humid atmospheres in the presence of CO_2 is presented in a separate paper.[13]

2. Experimental

Ceramic powder with composition $La_{0.2}Sr_{0.8}Fe_{0.79}Cr_{0.2}Mg_{0.01}O_3$ was bought commercially from Praxair Specialty Ceramics.[2] The powder was made by a spray pyrolysis process, and calcined at 1050 °C for 1–2 h. The samples were sintered at 1275 °C for 2 h in flowing N_2, to avoid cracking of the samples during heating and cooling. Sintered samples were found to be single phase with a cubic lattice parameter of 3.919 Å, giving a crystallographic density of approximately 92%. SEM analysis showed that Mg, as expected, gathered at the grain boundaries, thus inhibiting grain growth.

Sample pellets were cut into quarters which were placed in a sample holder of zirconia as shown in Fig. 1. Inert materials were used in the furnace internals, except for the furnace tube itself, which was made of XM metal.[3] The samples were exposed to 40% H_2O, 20% H_2 and 40% Ar at 1000 °C and 30 bar total pressure, corresponding to an equilibrium pO_2 of 10^{-14} bars. The total duration at the given test conditions varied from 1 to 500 h. Two additional experiments were conducted; one without the presence of humidity and one where XM metal coupon was placed in contact with the perovskite material.

All samples were examined visually and by Scanning Electron Microscopy (SEM) (Philips XL 30). Energy dispersive spectroscopy (EDS) was used to determine the compositions of various phases. The element concentrations of Sr, La, Fe, Cr and Si were normalized to 100 at% for clarity and easy comparison. X-ray diffraction (XRD) was used for phase identification on sample surfaces. The examination was performed on a Scintag PAD V diffractometer with a secondary graphite monochromator.

[2] Praxair Specialty Ceramics, Woodinville, WA 98072-6231.
[3] http://www.manoirusa.com/index.html.

3. Results

The main focus of the present investigation is the possible reaction between the perovskite and gaseous species in the ambient atmosphere. However, it should also be kept in mind that the perovskite is exposed to quite low oxygen potentials at high temperatures, so possible thermal decomposition into component oxides or even metallic phases may also become an issue. As stated in the previous section the samples are typically exposed to pO_2 equal to 10^{-14} bar at 1000 °C. Mizusaki et al.[7] reported that $La_{1-x}Sr_xFeO_{3-\delta}$ with $x = 0.6$ was stable even at 10^{-15} bar at 1000 °C. That is, it is likely that $La_{1-x}Sr_xFeO_{3-\delta}$ with $x = 0.8$ also is stable at the same conditions given that ca. 20% of Fe is substituted by Cr. According to Yokokawa et al.[8] $LaCrO_3$ is stable at less than 10^{-22} bar even at 1000 °C, emphasizing the stabilizing "power" of Cr in this material system. Thus it was assumed that the perovskites in question were stable at the prevailing oxygen chemical potentials and the possible deteriorating reactions were only due to reactions with species in the ambient atmosphere. This was also supported by XRD analysis which always showed that the perovskite compound was intact in the bulk of the sample (below the reaction layer) despite several hundred hours exposure at 1000 °C and at fairly low oxygen potentials (10^{-14} bar).

A white, Sr-rich layer is formed on the surface of the samples exposed to humid atmosphere at high temperature as shown in Fig. 2. The exposed parts of the sample were light colored and matte, whereas the part shielded by the sample holder was shiny and black as before exposure. The amount/thickness of the surface layer increased with time, followed by a reduction of the mechanical integrity of the specimens.

No reactions were found for the sample tested in dry atmosphere, and also no reaction was observed in the contact zone between a metal coupon and the sample. Reactions had occurred, however, at surfaces of the perovskite that were not in contact with the metal.

The new phase, strontium silicate, grew quite fast initially and already after 1 h the sample surface appeared quite differently as shown in Fig. 3(a).The new phase grew as needles increasing

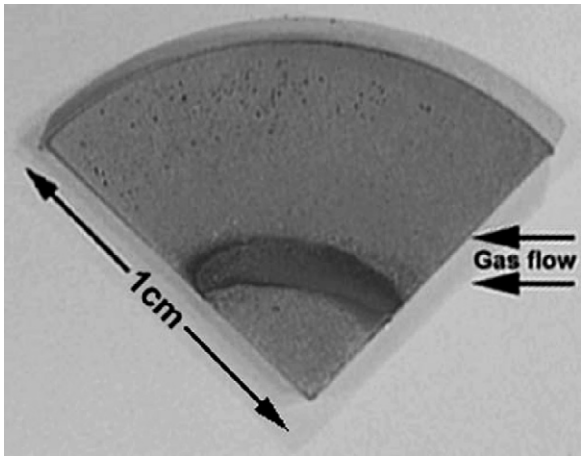

Fig. 2. Photo of sample after 500 h exposure at 1000 °C.

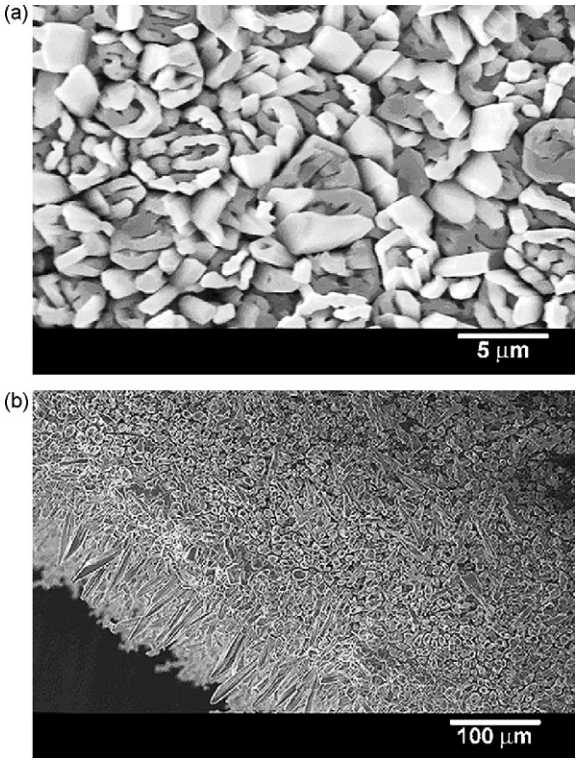

Fig. 3. (a) SEM micrograph of the surface after 1 h exposure at 1000 °C. (b) SEM micrograph of the surface after 500 h exposure at 1000 °C.

in length with time, and after 500 h needles as long as 100 μm were observed as shown in Fig. 3(b).

The identification of Sr_2SiO_4 was not trivial, as the presence of Si was unexpected, and in addition the Sr L_α and the Si K_α peaks are close (1.8066 and 1.7398 keV, respectively). Infrared (IR) spectroscopy analysis on the surface layer gave a first indication that a low atomic number oxide was present, before EDS analysis revealed a Sr–Si phase with a Sr:Si ratio of 2:1 in the surface layer. Rietveld analysis performed on the XRD data of the surface layer confirmed the presence of Sr_2SiO_4, both in the monoclinic and the orthorhombic modifications. Data from the Rietveld analysis were used to model the IR spectra, yielding a result in accordance with the collected IR spectra.

SEM micrographs of the cross sections of the samples are shown in Fig. 4. An outer Sr and Si-rich layer was demonstrated to be fairly dense (region I). This surface layer became more porous with time and detached easily after long exposures. Degradation of the perovskite near the surface following the preferential growth of Sr_2SiO_4 may explain the increased porosity near the original surface. A porous, Sr-depleted zone was observed beneath the original surface of the samples (region II). The original surface was at the border between regions I and II. Before reaching the bulk material, there was a transition zone where the grain boundaries were depleted in Sr (and Fe) and enriched in La and Cr and a secondary dark, Fe-, Cr- (and Mg-)rich phase was observed in addition to bulk perovskite materials in the original grains (region III). EDS spot analysis of the three phases are given in Table 1.

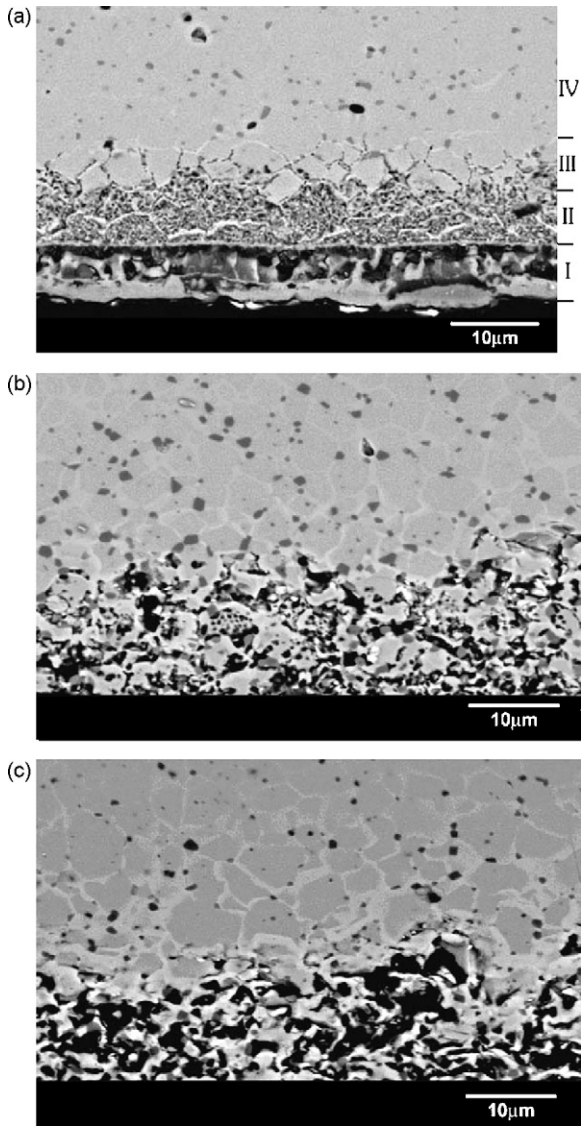

Fig. 4. (a) SEM micrograph of sample cross section after 4 h exposure at 1000 °C. The following regions are identified: (I) surface reaction layer, (II) porous Sr-depleted layer, (III) transition zone and (IV) Bulk. (b). SEM micrograph of sample cross section after 100 h exposure at 1000 °C. (c). SEM micrograph of sample cross section after 500 h exposure at 1000 °C.

EDS line scans confirmed the results of the spot analysis, as shown in Fig. 5. The porous layer (II) was depleted in Sr and to some extent also in Fe and enriched in Cr and La, while the Si content decreased from a high value at the surface to zero at the end of the porous layer. In the transition zone (III) the Sr content increased and the Cr and La contents decreased, while the Fe content had a maximum value in the transition zone.

Table 1
Elemental analysis of different phases observed in exposed specimens (at%)

Analysis spots	Sr	La	Fe	Cr	Mg
Dark gray spots	7	6	35	44	8
Grain boundaries	28	19	34	19	0
Grains	40	8	42	10	0

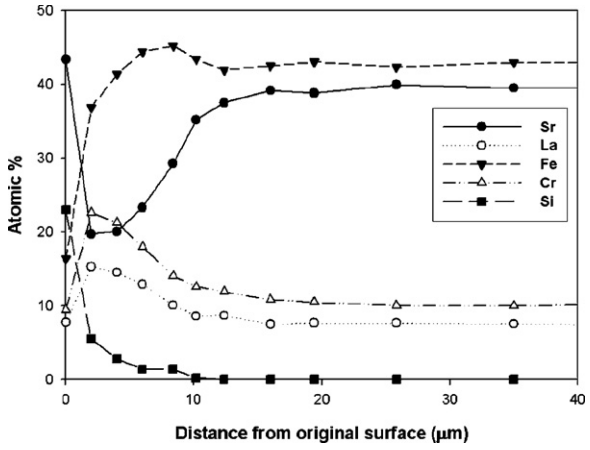

Fig. 5. Elemental analysis of regions II–IV after 4 h exposure. The analysis was taken along 100 μm long lines at distances from 0 to 25 μm from the original surface, along 200 μm long lines at distances from 30 to 75 μm and along 400 μm long lines from 75 to 150 μm inwards from the original surface due to different magnifications.

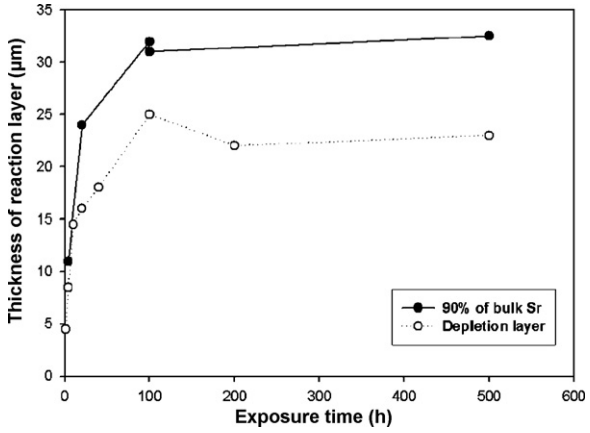

Fig. 6. The thickness of porous, Sr-depletion layer (II) and reaction layer, defined as distance from original surface to level where concentration of Sr reaches 90% of bulk Sr concentration, as a function of time at 1000 °C.

EDS line scans were used to determine the extent of reaction by measuring the distance from the surface to the line where the Sr content had reached 90% of the Sr-bulk content. The extent of the reaction was also quantified by measuring the distance from the original surface to the end of the porous, Sr-depleted layer (II) on SEM images of sample cross section. Both methods gave the same trend in the extent of reaction versus exposure time as shown in Fig. 6. The thickness of the Sr-depleted layer increased with increasing exposure up to 100 h, though not linearly, before it leveled off. The reproducibility of the EDS line scan analysis was good, as seen at 100 h exposure where two different areas on the cross section have been examined.

4. Discussion

The vaporization of SiO_2 at high temperatures and pressures is known from other applications, and gas phase transport of SiO_x species have been found to occur by two different mechanisms:

(i) Evaporation of SiO under reducing (H_2) conditions[10]:

$$SiO_2(s) + H_2(g) \leftrightarrow SiO(g) + H_2O(g) \quad (1)$$

or

$$SiO_2(s) \leftrightarrow SiO(g) + 0.5O_2(g) \quad (2)$$

(ii) Reactions with steam at high pressure to form $SiO_2{\cdot}2.5H_2O$[11]:

$$SiO_2(s) + 2.5H_2O(g) \leftrightarrow SiO_2{\cdot}2.5H_2O(g) \quad (3)$$

The consequence of reaction (3) is that SiO_2 can be transported through the gas phase also under oxidizing and humid conditions. The mechanism is known from steam reforming processes. The solubility of silica in water vapor increases with increasing temperature and pressure.[15] SiO_2 may easily form on the surface of metals containing Si when exposed to air, or it may form at high partial pressures of steam at high temperature by a reaction of steam with Si metal:

$$Si(s) + 2H_2O(g) \leftrightarrow SiO_2(s) + 2H_2(g) \quad (4)$$

This reaction will provide a continuous supply of SiO_2 on the surface of the furnace tube material, hence providing a continuous supply of SiO_2 available for gasification through reactions (1)–(3).

In the mechanism described by Eqs. (1) and (2), the vapor pressure of SiO at 1000 °C, $pO_2 = 10^{-14}$ bar and total pressure of 30 bar is 10^{-12} bar.[14] Under the operating conditions in this experiment this corresponds to 6×10^{-8} wt ppm SiO(g). Using Eq. (3) a solubility of 200 wt ppm silica in superheated steam at 1000 °C and 30 bar can be estimated through extrapolation of the data from Straub.[16] The amounts of Sr_2SiO_4 observed correspond to rather high rates of gas phase transport of SiO_2, and the gas phase transport is more appropriately described by transport of SiO_2 as a hydrated species as given in reaction (3) than by the minute partial pressure of SiO(g) corresponding to equilibria established by reactions (1) and (2), respectively. The mechanism of transport of SiO_2 as a hydrated species was supported by the fact that no reaction was observed on the perovskite surface either in dry atmosphere or in direct contact with the XM metal.

There are a number of different compounds that may form in Sr–Si–O system, depending on the Sr:Si ratio.[17] XRD data revealed Sr_2SiO_4 in the surface layer after 500 h exposure. Formation of Sr_2SiO_4 at the surface was confirmed by EDS analysis of the white surface layer which showed a Sr–Si rich phase with a Sr:Si ratio of 2:1. This is not consistent with what was reported by Viitanen et al.[9] They did not, however, support their data with XRD analysis to identify the phase, and only reported a Sr enriched surface. Hence, it is likely that they also have Sr_2SiO_4 and not pure SiO_2.

The following equation shows a possible reaction for the formation of Sr_2SiO_4:

$$La_{0.2}Sr_{0.8}Fe_{0.79}Cr_{0.2}Mg_{0.01}O_3 + ySiO_2{\cdot}2.5H_2O \rightarrow ySr_2SiO_4 + \text{Sr-depleted } La_{0.2}Sr_{0.8}Fe_{0.79}Cr_{0.2}Mg_{0.01}O_3 + 2.5yH_2O \quad (5)$$

When the Sr depletion of the perovskite has progressed far enough, the perovskite will convert to a different structure in the same manner as was described for CO_2 degradation.[13]

The micrographs shown in Fig. 4 have several interesting features. Initially, the grain boundaries seemed to be chemically modified due to the presence of SiO_2 at the surface. The grain boundaries were depleted in Sr, leaving a La-Cr rich phase. A secondary Fe- and Cr-rich phase, seen as dark grey spots on the micrographs, was found throughout the examined section, preferentially close to the grain boundaries. With time the concentration of the Fe- and Cr-rich secondary phase was more prominent, especially in the transition zone, The thickness of the La–Cr rich grain boundary phase increased with time, and after 100 h formed a continuous network in the transition zone. The formation of a continuous grain boundary phase may significantly slow down the transport of Sr to the surface, consistent with the measured extent of reaction given in Fig. 6 which shows a passivation trend above 100 h exposure. After 500 h, the darker Fe- and Cr-rich phase was almost completely gone, both from the bulk region (IV) and from the edge of the porous Sr-depleted zone (II/III). The porosity of the transition zone (III) was also considerably higher than for shorter exposure times. The increased porosity and disappearance of the Fe- and Cr-rich phase may be explained by rearrangement reactions that took place once the passivation stage was reached. The compositions of the three phases did not change considerably from those reported in Table 1.

Based on the observed behavior, a possible reaction mechanism can be summed up by the following points:

- SrO at the surface reacted with SiO_2 transported through the gas phase as a silica hydrate to form Sr_2SiO_4 at the surface.
- Sr, and to a certain degree Fe, was transported along the grain boundaries towards the surface. It is likely that the initial main source of Sr was at the grain boundaries, explaining the preferential degradation of the grain boundaries in the first few hours of exposure. When most Sr and Fe had left the grain boundaries, Sr and Fe were drawn from the grains, creating porous grains.
- Initial degradation of the grains in the transition zone (III) depleted the structure with respect to Sr and Fe, creating a thicker $LaCrO_3$ rich grain boundary. As the grain boundary region thickened and the width of the transition zone (III) increased, the Sr transport rate to the surface decreased.

5. Conclusions

SiO_2 evaporated from the furnace tube surface was found to react with SrO in the perovskite $La_{0.2}Sr_{0.8}Fe_{0.79}Cr_{0.2}Mg_{0.01}O_3$ to form Sr_2SiO_4 on the surface of the perovskite material in humid atmospheres at high temperature and pressure. SiO_2 transport depended on formation of a gaseous silica hydrate and hence on the presence of water vapor. Passivation was observed to occur after approximately 100 h exposure. No reactions were observed either under dry conditions or when shielding the Si-source. When using Sr-based perovskite materials in membrane reactors it is of importance to avoid Si-sources (Si containing alloys, insulation materials, sealing materials) in the vicinity of the membrane at high steam partial pressures and high temperatures.

Acknowledgments

This report was written with support of the U.S. Department of Energy under Contract No. DE-FC26-01NT41096. The Government reserves for itself and others acting on its behalf a royalty-free, nonexclusive, irrevocable, worldwide license for Governmental purposes to publish, distribute, translate, duplicate, exhibit and perform this copyrighted presentation. We acknowledge DoE for financial support to the OTM (Oxygen Transport Membranes) Alliance (Praxair, BP, Amoco, Sasol, and Statoil). The authors acknowledge collaboration and fruitful discussions with partners in the OTM Alliance. Thanks to BP for supplying some of the samples, and to J.A. Kaduk at BP Amoco for careful XRD analysis of sample surfaces and identification of the surface coating after 500 h as two polymorphs of Sr_2SiO_4. We also appreciated assistance with SEM analysis by Sten Egil Johnsen.

References

1. Balachandran, U., Dusek, J. T., Sweeney, S. M., Poeppel, R. B., Mieville, R. L., Maiya, P. S. *et al.*, Methane to syngas via ceramic membranes. *Am. Ceram. Soc. Bull.*, 1995, **74**(1), 71–75.
2. Robinson, E. T., Aasland, S. and Chen, C. C., The application of oxygen transport membranes for syngas or hydrogen production. In *AIChE spring meeting*, April 26, 2004, Session T9008, Paper 68d.
3. Robinson, E. T., Oxygen transport membranes for ultra-clean transportation fuel production. In *225th National meeting ACS, March 2003, Fuel Chemistry Div., Paper, Session Advances in Membranes for Energy and Fuel Applications*. Paper 161.
4. Foster, E. P., Tijm, P. J. A. and Bennett, D. L., Advanced gas-to-liquids processes for syngas and liquid-phase conversion. *Nat. Gas Convers. V Stud. Surf. Sci. Catal.*, 1998, **119**, 867–874.
5. Udovich, C. A., Ceramic membrane reactors for the conversion of natural gas to syngas. *Nat. Gas Conv. V Stud. Surf. Sci. Catal.*, 1998, **119**, 417–422.
6. Martin, M., Materials in thermodynamic potential gradients. *Pure Appl. Chem.*, 2003, **75**(7), 889–903.
7. Mizusaki, J., Yoshihiro, M., Yamauchi, S. and Fueki, K., Nonstoichiometry and defect structure of the perovskite-type oxides $La_{1-x}Sr_xFeO_{3-\delta}$. *J. Solid State Chem.*, 1985, **58**, 257–266.
8. Yokokawa, H., Sakai, N., Kawada, T. and Dokiya, M., Thermodynamic stabilities of perovskite oxides for electrode and other electrochemical material. *Solid State Ionics*, 1992, **52**(1–3), 43–56.
9. Viitanen, M. M., v. Welzenis, R. G., Brongersma, H. H. and van Berkel, F. P. F., Silica poisoning of oxygen membranes. *Solid State Ionics*, 2002, **150**, 223–228.
10. Shick, H. L., A thermodynamic analysis of the high-temperature vaporization properties of silica. *Chem. Rev.*, 1960, **60**(4), 331–362.
11. Huggett, L. G. and Piper, L., Transfer of silica in the pressure steam reforming process. In *Materials technology in steam reforming processes*, ed. C. Edeleau. Pergamon Press, London, 1966, pp. 337–342.
12. Kaus, I., Wiik, K., Kleveland, K., Krogh, B. and Aasland, S., Oxygen transport properties in $La_{1-x}SrxFe_{1-y}MyO_{3-\delta}$ (M = Cr, Ti). *Solid State Ionics*, 2007, **178**, 817–826.

13. Kaus, I., Wiik, K., Dahle, M., Hofstad, K. H. and Aasland, S., Stability of $SrFeO_3$ based materials in H_2O/CO_2 containing atmospheres at high temperatures and pressures. *J. Am. Ceram. Soc.*, in press.
14. *JANAF thermodynamical tables*, 3rd ed., J. Phys. Chem. Ref. Data, *Vol 14* (Suppl. 1), 1985.
15. Kennedy, G. C., The hydrothermal solubility of silica. *Econ. Geol.*, 1944, **39**, 25–36.
16. Straub, F. G., Steam turbine blade deposits. *Univ. Ill. Eng. Exp. Station Bull. Ser.*, 1946, 364.
17. *Phase diagrams for ceramists*. American Ceramic Society, Westerville, OH.